Staggered Finite Difference Schemes for Balance Laws

Gabriella Puppo and Giovanni Russo

Abstract. In this paper a new family of high-order finite-difference shock-capturing central schemes for hyperbolic systems with stiff source is presented. The schemes are based on recently developed finite difference discretization on staggered grids, coupled with implicit-explicit (IMEX) time discretization for an efficient treatment of the source term. Numerical tests show the robustness and accuracy of the method, for a wide range of the stiffness parameter.

1. Introduction

Finite difference (FD) schemes are usually preferred to finite volume (FV) schemes for constructing high-order shock-capturing methods for balance laws [8]. These schemes are often based on a method-of-line approach: space is discretized by finite difference, and high order non oscillatory properties are usually obtained by the choice of a monotone flux and a non oscillatory reconstruction such as essentially non oscillatory (ENO) or weighted essentially non oscillatory (WENO) [12]. The original system is approximated by a set of ode's for the pointwise value of the unknown field at the center of each cell. At this point, an implicit-explicit (IMEX) time discretization can be applied to the resulting set of ode's [1], [8], [3].

For systems of conservation laws, finite volume shock-capturing central schemes have been constructed both on staggered [6], [5], and unstaggered [4]. A review on central schemes can be found, for example, in [13].

The central approach has the advantage of providing an automatic dissipative mechanism that, when used in conjunction with a suitable non oscillatory reconstruction, yields to a non oscillatory scheme, without the requirement of an explicit knowledge of the characteristic structure of the system. The use of characteristic information, however, may improve the overall performance of the scheme, by eliminating the oscillations that otherwise appear when the reconstruction is performed in conservative variables. This effect is studied in [7].

Staggered schemes present a sharper resolution compared to their unstaggered counterpart (based on local Lax-Friedrichs flux), and it is therefore interesting to construct a finite difference version of the high order central schemes, with the aim of solving systems of balance laws. A comparison between staggered and non staggered finite volume central scheme is presented in [10]. That paper also shows that staggered schemes are slightly less sensitive to the use of characteristic variables in the reconstruction.

A family of shock-capturing finite-difference central schemes has been recently constructed [9]. In the same paper a comparison is performed between staggered and unstaggered FV and FD schemes for some test cases in one space dimension. All these schemes give comparable results for the same mesh. Staggered schemes appear to be more accurate, but slightly more expensive than their unstaggered counterpart; because they require a larger number of time steps, due to the more restrictive CFL condition that imposes that the time step is about half of the time step required for unstaggered schemes. The larger number of steps is partially compensated by the lack of need of a numerical flux function, which makes one staggered time step quite less expensive than the unstaggered one.

In this paper we show how to couple finite difference central discretization with IMEX time discretization, making use of recently developed central Runge-Kutta approach [7].

Next section two is devoted to the construction of FD-CRK-IMEX schemes, and in the last section we present some numerical results.

2. Description of the scheme

In this section, we describe the construction of finite difference schemes based on staggered cells for balance equations. Consider the system of balance laws:

$$u_t + f_x(u) = \frac{1}{\epsilon} g(u). \tag{1}$$

Here, $u(x,t)$ is a function from $\mathbb{R} \times \mathbb{R}^+$ to $\mathbb{R}^m$, f and g are functions from $\mathbb{R}^m$ to $\mathbb{R}^m$, and $\epsilon \geq 0$ is the stiffness parameter. Moreover, we suppose that the Jacobian of f has real eigenvalues and a complete set of eigenvectors for each (x,t).

We are considering relaxation systems, i.e. systems of equations that, when $\epsilon \to 0$, reduce to a smaller system of conservation laws [2].

2.1. Finite difference schemes on staggered grids

In the construction of finite difference schemes on staggered grids, we cover the computational domain with grid points of the form (x_j, t^n) for even values of n, while, for odd values of n we consider a staggered grid, with grid points of the form $(x_{j+1/2}, t^n)$, with $x_{j+1/2} - x_j = h/2$.

The evolution of the point values of the solution u on the staggered grid points is given by:

$$\frac{d}{dt}u_{j+1/2}(t) = -\frac{1}{h}\left(\hat{f}(u(x_{j+1},t)) - \hat{f}(u(x_j,t))\right) + \frac{1}{\epsilon}g(u(x_{j+1/2},t)), \tag{2}$$

where $\hat{f}$ denotes the cell primitive of the physical flux f, in the sense that:

$$\begin{aligned} f(u(x_j,t)) &= \tfrac{1}{h}\int_{x_j-h/2}^{x_j+h/2}\hat{f}(u(x,t))\,dx \\ &\implies \partial_x f(u)|_{x_j+h/2}(t) = \tfrac{1}{h}\left[\hat{f}(u(x_j+h,t)) - \hat{f}(u(x_j,t))\right]. \end{aligned}$$

Thus the evolution equation for the point values is automatically written in conservation form. This approach for the FD scheme on unstaggered grid was introduced in [11].

As is common to central schemes on staggered grids, see [13, 6, 5], the main idea is to construct piecewise polynomial interpolants which are smooth in the intervals I_j centered around the grid points x_j on which the numerical solution is known. Thanks to grid staggering, the numerical fluxes need to be computed at the points x_j, where the interpolants are smooth. For this reason, the flux splitting required in standard FD schemes, see again [11], is not necessary in the present case.

System (2) is first discretized in time, with a IMEX Runge-Kutta scheme. The numerical solution (pointwise value of the solution at the center of the staggered cell) is given by

$$u_{j+1/2}^{n+1} = u_{j+1/2}^{n} + \Delta t\sum_{i=1}^{\nu}\frac{\tilde{b}_i}{h}\left(\hat{f}(u^{(i)}(x_{j+1})) - \hat{f}(u^{(i)}(x_j))\right) + \frac{\Delta t}{\epsilon}\sum_{i=1}^{\nu} b_i g(u^{(i)}(x_{j+1/2})), \tag{3}$$

where $u^{(i)}(x_j)$ denotes the i-th stage value of the IMEX scheme [8]. Since the numerical solution is smooth at x_j, if the time step is small enough, the intermediate states $u^{(i)}$ can be computed using the differential form of the PDE:

$$\partial_t u = -\partial_x f(u) + \frac{1}{\epsilon}g(u), \tag{4}$$

following the CRK approach proposed in [7]. Thus the quantities $u^{(i)}$ are obtained by the formula for the stage values of an IMEX Runge-Kutta, applied to Eq.(4) as follows:

$$u^{(i)}(x_j) = u_j^n - \Delta t\sum_{k=1}^{i-1}\tilde{a}_{i,k}\partial_x f(u^{(k)})|_j + \frac{\Delta t}{\epsilon}\sum_{k=1}^{i} a_{i,k}g(u_j^{(k)}), \tag{5}$$

where $\tilde{a}_{ij}$ and a_{ij} denote the coefficients of the explicit and implicit RK schemes, respectively. We assume that the implicit scheme is diagonally implicit.

Equations (3) and (5) completely define the time discretization of (2). Let us now turn to the space discretization. The first task is to evaluate the term $u_{j+1/2}^n$ on the RHS of (3). This is done through deconvolution. First, we solve the following interpolation problem: given a smooth function $u(x)$, compute a non-oscillatory

piecewise polynomial approximation to the primitive of u. More precisely, find a piecewise polynomial non oscillatory function $v(x)$ such that:

$$v = \mathsf{shift}(u) \quad : \quad \begin{array}{ll} 1) & u(x_j) = \frac{1}{h}\int_{x_{j-1/2}}^{x_{j+1/2}} v(x)\,dx \quad \forall j \\ 2) & \frac{1}{h}\int_{x_j}^{x_{j+1}} v(x) = u(x_{j+1/2}) + O(h^r), \end{array} \tag{6}$$

where r is the accuracy of the scheme. This problem can be solved using the central WENO reconstruction of [5]. Thus, given the point values of the numerical solution u_j^n, we compute the cell primitive $v(x)$, and we set:

$$u_{j+1/2}^n = \frac{1}{h}\int_{x_j}^{x_{j+1}} v(x)\,dx.$$

Next, at each stage value, we need to evaluate the x derivative of f, starting from its point values. Again, this is an interpolation problem, that can be framed as follows. Given a smooth function $U(x)$, find a piecewise polynomial non oscillatory function $v(x)$ such that:

$$v = \mathsf{derivative}(U) \quad : \quad \begin{array}{ll} 1) & U(x_j) = v(x_j) \quad \forall j \\ 2) & \frac{dv}{dx}|_{x_j} = \frac{dU}{dx}|_{x_j} + O(h^{r-1}), \end{array} \tag{7}$$

where r is the accuracy of the scheme, see again [5]. In the present case, at each stage value $i = 1, \ldots, \nu - 1$, identify $U(x_j) := f(u_j^{(i)})$ and apply the above reconstruction to the point values $U(x_j)$.

Since t

Note that accuracy of order $r - 1$ is sufficient, since he stage values are computed only locally, and an accuracy of order $O(h^{r-1})$ is enough to guarantee global accuracy of $O(h^r)$.

At the i-th stage value, we need to solve, in general, a non linear system of algebraic equations. Because of the diagonally implicit structure of the scheme, only a $m \times m$ nonlinear system has to be solved at each stage in each cell.

Finally, we need to update the solution, computing the RHS of (3). This requires two steps. First, starting from the data $f(u_j^{(i)})$ we need to compute the primitive of the flux $\hat{f}(u_j^{(i)})$. This again can be framed as the following interpolation problem.

Let $F(x)$ be a smooth function, and let $\hat{F}$ be its cell primitive. Find a piecewise polynomial non oscillatory function $v(x)$ such that:

$$v = \mathsf{primitive}(F) \quad : \quad \begin{array}{ll} 1) & F(x_j) = \frac{1}{h}\int_{x_{j-1/2}}^{x_{j+1/2}} v(x)\,dx \quad \forall j \\ 2) & v(x_j) = \hat{F}(x_j) + O(h^r). \end{array} \tag{8}$$

For a second order accurate scheme, this step is not necessary, because $U(x_j) = \hat{U}(x_j) + O(h^2)$. For the fourth order accurate scheme, instead, a reconstruction step is needed. We use again the Central WENO reconstruction.

The second step consists in shifting the evaluation of the source term. After the evaluation of the stage values $u_j^{(i)}$, one immediately computes the values of the

source term at the grid points, namely $g(u_j^{(i)})$. But the RHS of (3) requires instead $g(u_{j+1/2}^{(i)})$. To obtain these data, we identify $U(x_j) = g(u_j^{(i)})$ and we apply the reconstruction (6).

Remark. The description given above permits to construct high order finite difference schemes for balance laws. It is clear that, as stated, the scheme just described requires a very large number of reconstruction steps. However the complexity of the scheme can be drastically reduced, if a non linear reconstruction is used only once per time step. It has already been shown in several tests, see [10] and [9] that to prevent the onset of spurious oscillations it is enough to compute the non linear weights appearing in the reconstruction only once per time step. If this approach is followed, then it is easy to prove that it is enough to compute the primitive of the flux and the shift in the source term only once per time step.

3. Numerical results

We have performed an investigation and a comparison between high order finite difference schemes on staggered and unstaggered grids in [9]. Here we concentrate on the properties of finite difference schemes on staggered grids.

Convergence study. The convergence of our schemes was studied with the aid of two smooth solutions of the Broadwell model of rarefied gas dynamics [8]. The model is of the form (1), with $u = (\rho, m, z)$, $f = (m, z, m)$, $g = (0, 0, (\rho^2 + m^2 - 2\rho z)/2)$.

The equilibrium state is $z = z_E = (\rho^2 + m^2)/(2\rho)$. Thus, as $\epsilon \to 0$, this system reduces to a 2×2 quasilinear system of conservation laws for ρ and m. We consider the smooth and periodic initial data $\rho_0(x)$, $v_0(x)$, $z_0(x)$ given by:

$$\rho_0 = 1 + a_\rho \sin(\frac{2\pi x}{L}), \quad v_0 = \frac{1}{2} + a_v \sin(\frac{2\pi x}{L}), \quad z_0 = a_z \frac{1}{2} \left(\rho_0 + \rho_0 v_0^2\right),$$

where $v(x,t) = m(x,t)/\rho(x,t)$ is the velocity. The computational region is $L = 20$. The system has eigenvalues $\mu = 0, \mu = \pm 1$, thus the mesh ratio λ was chosen as $\lambda = 0.9/2$. The computation was stopped at $T = 20$. We used two sets of parameters:

$$\text{i) } a_\rho = 0.3,\ a_v = 0.1,\ a_z = 1.0; \qquad \text{ii) } a_\rho = 0.3,\ a_v = 0.1,\ a_z = 0.2.$$

In the first case, the system starts out in local equilibrium, i.e. $g(u_0) = 0$, while in the second case the system is not at local equilibrium initially, so that an initial layer forms between the initial data and the solution of the relaxed system for small values of ϵ, and this may slow down convergence.

Table 1 show the relative errors in the $L1$ norm for the density in the case with initial layer. The results without an initial layer are very similar, and have been omitted. All data shown refer to the third order IMEX3 scheme developed in [8]. For values of ϵ smaller than 10^{-6}, the error remains approximately constant. There is no apparent deterioration in accuracy when an initial layer is present.

L^1 norm of the error with initial layer							
N	$\epsilon = 1$	$\epsilon = 10^{-1}$	$\epsilon = 10^{-2}$	$\epsilon = 10^{-3}$	$\epsilon = 10^{-4}$	$\epsilon = 10^{-5}$	$\epsilon = 10^{-6}$
50	1.927E-6	9.003E-6	2.583E-5	2.076E-5	2.014E-5	2.012E-5	2.012E-5
100	1.610E-7	7.971E-7	2.841E-6	2.153E-6	1.290E-6	1.279E-6	1.278E-6
200	1.700E-8	1.308E-7	2.265E-7	6.175E-7	1.104E-7	8.288E-8	8.289E-8
400	2.070E-9	1.939E-8	3.963E-8	2.018E-7	3.120E-8	6.487E-9	6.499E-9

TABLE 1. L^1 error on cell averages for IMEX3 scheme

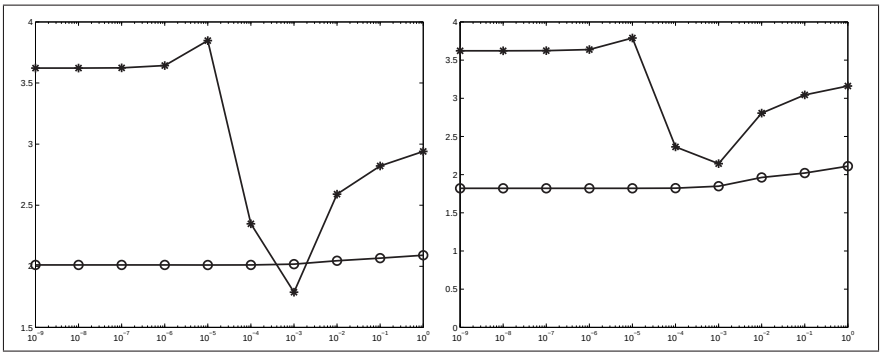

FIGURE 1. Order of accuracy as a function of ϵ on Broadwell's model, for the second order (o) and the third order (*) IMEX schemes. On the left, no initial layer, on the right, with initial layer

$$\begin{array}{c|cc} 0 & 0 & 0 \\ 1 & 1 & 0 \\ \hline & 1/2 & 1/2 \end{array} \qquad \begin{array}{c|cc} \gamma & \gamma & 0 \\ 1 & 1-2\gamma & \gamma \\ \hline & 1/2 & 1/2 \end{array} \qquad \gamma = 1 - \frac{1}{\sqrt{2}}$$

TABLE 2. Second order IMEX scheme

Fig. 1 displays the accuracy as a function of the stiffness parameter ϵ for the second and third order IMEX shemes described in this work.

The second order scheme (labelled in the figure with the empty circles) uses the IMEX method defined in Table 2 and a second order piecewise linear reconstruction in space, with the MinMod limiter. Its accuracy is almost second order uniformly with respect to ϵ. There is only a slight deterioration in accuracy for small values of ϵ when an initial layer is present. Probably, the MinMod limiter in this case causes an irretrievable loss of information.

The higher order scheme uses the IMEX method specified in Table 3 and the fourth order Central WENO reconstruction of [5]. The figure shows a deterioration in accuracy for moderately stiff values of ϵ. Accuracy actually increases, when the

0	0	0	0	0
0	0	0	0	0
1	0	1	0	0
1/2	0	1/4	1/4	0
	0	1/6	1/6	2/3

α	α	0	0	0
0	$-\alpha$	α	0	0
1	0	$1-\alpha$	α	0
1/2	β	η	$1/2-\beta-\eta-\alpha$	α
	0	1/6	1/6	2/3

$\alpha = 0.24169426078821, \qquad \beta = 0.06042356519705, \qquad \eta = 0.1291528696059$

TABLE 3. Third order IMEX scheme

Broadwell model relaxes towards the Euler equations of isentropic gas dynamics. Note that here the scheme is more than third order accurate, probably because the space discretization is fourth order accurate.

A Riemann problem. We now study a Riemann problem to assess the non oscillatory properties of our schemes. We consider the following set of initial data:

$$\begin{pmatrix} \rho \\ m \\ z \end{pmatrix}(x, t=0) = \begin{cases} [2, \quad 1, \quad 1]^T & x < 0.2 \\ [1, \quad 0.13962, \quad 1]^T & x \geq 0.2 \end{cases}$$

The computational domain is $[-1, 1]$, with periodic boundary conditions. The mesh ratio $\lambda = 0.25$, and the final time is $T = 0.5$. The results obtained for $N = 200$ grid points appear in Fig. 2 for several values of ϵ. The reference solution (solid line) was obtained with the third order IMEX3 scheme and 1000 grid points.

It is apparent from the figure, that the scheme produces an essentially non-oscillatory numerical solution, for all values of ϵ considered. Also, the higher order scheme exhibits a better resolution of discontinuities. For a comparison, see [8].

References

[1] U. Asher, S. Ruuth, R. J. Spiteri, *Implicit-explicit Runge-Kutta methods for time dependent Partial Differential Equations*, Appl. Numer. Math. 25, (1997), pp. 151–167.

[2] G. Q. Chen, C. D. Levermore and T.-P. Liu, Hyperbolic conservation laws with stiff relaxation terms and entropy, Comm. Pure Appl. Math. **47** (1994), no. 6, 787–830.

[3] Kennedy C. A., Carpenter M. H., *Additive Runge-Kutta schemes for convection-diffusion-reaction equations*, Appl. Math. Comp., (2002).

[4] Kurganov A., Tadmor E., *New high-resolution central schemes for nonlinear conservation laws and convection-diffusion equations*, J. Comput. Phys. **160** (2000), no. 1, 241–282.

[5] Levy D., Puppo G., Russo G., *Central WENO Schemes for Hyperbolic Systems of Conservation Laws*, Math. Model. and Numer. Anal., **33**, no. 3 (1999),

[6] Nessyahu H., Tadmor E., *Non-oscillatory Central Differencing for Hyperbolic Conservation Laws*, J. Comput. Phys., **87**, no. 2 (1990), 408–463. 547–571.

[7] Pareschi L., Puppo G., Russo G., *Central Runge-Kutta Schemes for Conservation Laws*, in press on SIAM J. Sci. Comp.

[8] Pareschi L., Russo G., *Implicit-explicit Runge-Kutta schemes and applications to hyperbolic systems with relaxation*, accepted on Journal of Scientific Computing.

[9] Puppo G., Russo G., *Staggered finite difference schemes for conservation laws*, in preparation.

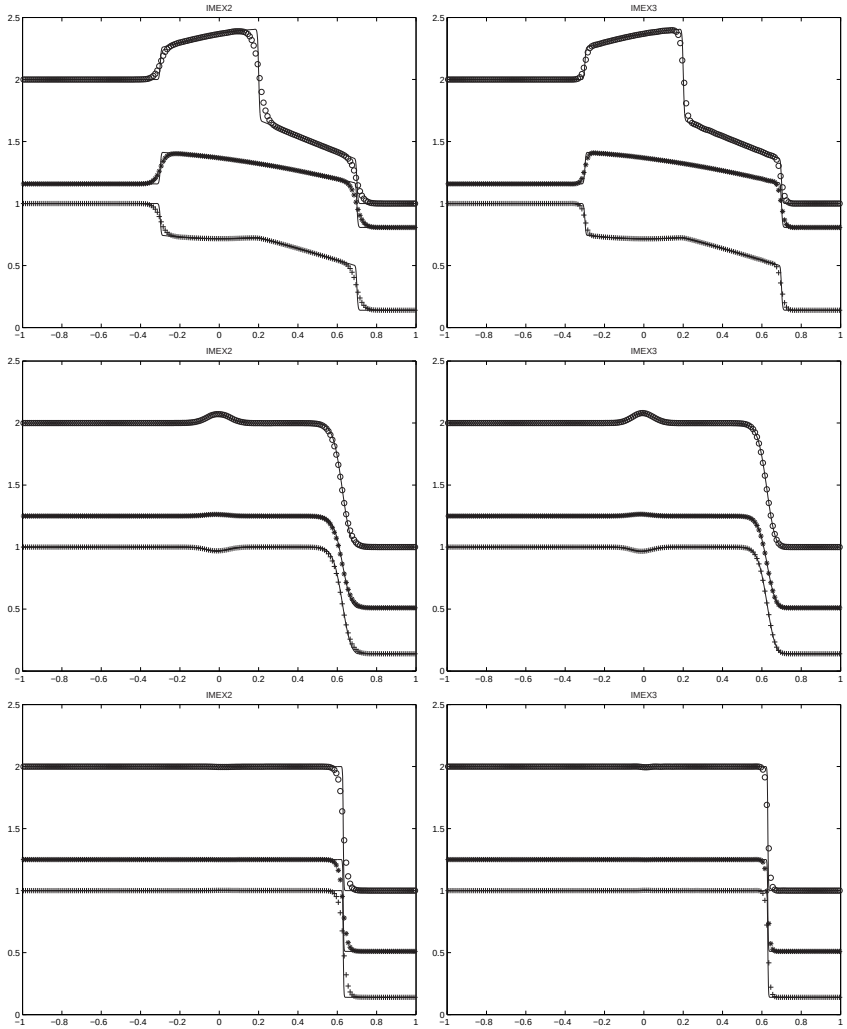

FIGURE 2. Riemann problem for Broadwell's model, for the second order (left) and the third order (right) IMEX schemes. From top to bottom: $\epsilon = 1$, $\epsilon = 0.02$ and $\epsilon = 10^{-8}$. Each plot contains the three components: ρ (o), m (+) and z (*).

[10] Qiu J, and Shu C.W., *On the construction, comparison, and local characteristic decomposition for high order central WENO schemes*, J. Comput. Phys., **175** (1), 2002, 108–127.

[11] Shu C.-W., Osher S., *Efficient Implementation of Essentially Non-oscillatory Shock-Capturing Schemes*, JCP **77**, 1988, 439-471.

[12] Shu C.-W., *Essentially Non-Oscillatory and Weighted Essentially Non-Oscillatory Schemes for Hyperbolic Conservation Laws* in Advanced Numerical Approximation of Nonlinear Hyperbolic Equations, Lecture Notes in Mathematics (A. Quarteroni editor), Springer, Berlin, 1998.

[13] Tadmor E., *Approximate Solutions of Nonlinear Conservation Laws*, in Advanced Numerical Approximation of Nonlinear Hyperbolic Equations, Lecture Notes in Mathematics (editor: A. Quarteroni), Springer, Berlin, 1998.

Dipartimento di Matematica, Politecnico di Torino
Corso Duca degli Abruzzi 24, 10129 Torino, Italy
E-mail address: gabriella.puppo@polito.it

Dipartimento di Matematica ed Informatica, Università di Catania
Viale Andrea Doria 6, 95125 Catania, Italy
E-mail address: russo@dmi.unict.it